

Atomistic Model for the Polyamide Formation from β -Lactam Catalyzed by *Candida antarctica* Lipase B

Iris Baum,[†] Brigitta Elsässer,[†] Leendert W. Schwab,[†] Katja Loos,[†] and Gregor Fels^{*‡}

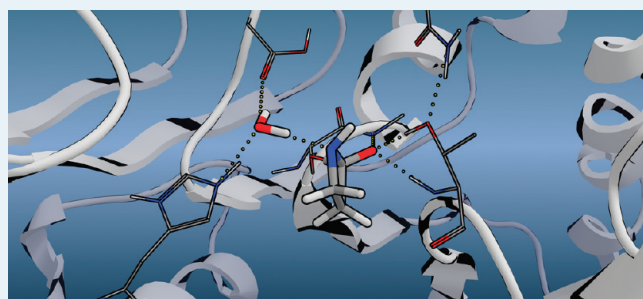
[†]Department of Chemistry, University of Paderborn, Warburger Strasse 100, D-33098 Paderborn, Germany

[‡]Department of Polymer Chemistry and Zernike Institute for Advanced Materials, University of Groningen, Nijenborgh 4, 9747, AG Groningen, The Netherlands

ABSTRACT: *Candida antarctica* lipase B (CALB) is an established biocatalyst for a variety of transesterification, amidation, and polymerization reactions. In contrast to polyesters, polyamides are not yet generally accessible via enzymatic polymerization. In this regard, an enzyme-catalyzed ring-opening polymerization of β -lactam (2-azetidinone) using CALB is the first example of an enzymatic polyamide formation yielding unbranched poly(β -alanine), nylon 3. The performance of this polymerization, however, is poor, considering the maximum chain length of 18 monomer units with an average length of 8, and the molecular basis of the reaction so far is not understood.

We have employed molecular modeling techniques using docking tools, molecular dynamics, and QM/MM procedures to gain insight into the mechanistic details of the various reaction steps involved. As a result, we propose a catalytic cycle for the oligomerization of β -lactam that rationalizes the activation of the monomer, the chain elongation by additional β -lactam molecules, and the termination of the polymer chain. In addition, the processes leading to a premature chain termination are studied. Particularly, the QM/MM calculation enables an atomistic description of all eight steps involved in the catalytic cycle, which features an in situ-generated β -alanine as the elongating monomer and which is compatible with the experimental findings.

KEYWORDS: *Candida antarctica* lipase B, enzyme catalysis, β -lactam ring-opening, molecular modeling, enzymatic polymerization, enzyme acylation



INTRODUCTION

Lipases have emerged from their metabolic use in ester cleavage of triglycerides to versatile biocatalysts that can be used for enantioselective hydrolysis of esters in water and for transesterification and transformation of esters to amides in organic solvents.¹ In addition, during the last 10 years, enzymes have also proven to be effective catalysts for polymerization reactions that proceed cost effectively with high regio-, enantio-, and chemoselectivity under relatively mild conditions.^{2,3} In this respect, *Candida antarctica* lipase B (CALB) immobilized on polyacrylic resin (Novozyme 435) is a particularly useful enzyme preparation because it shows exceptionally high stability and good activity in organic solvents, even at higher temperatures. Although CALB has successfully been employed for the synthesis of polyesters from linear^{4–8} and cyclic^{9–15} starting materials, little has been reported on the preparation of polyamides catalyzed by enzymes.^{16,17}

Schwab et al. have recently described the first approach for a synthesis of unbranched poly(β -alanine), nylon 3, by enzymatic ring-opening polymerization starting from unsubstituted β -lactam (2-azetidinone, β -propiolactam).¹⁸ The polymerization, however, proceeds with poor yield and with a maximum chain length of only 18 units and an average length of 8. Therefore, an optimization of the process is still necessary to produce a polymer for industrial use. This is, indeed, desirable because it

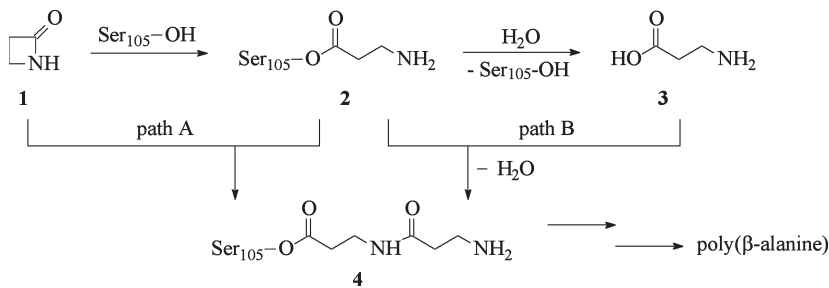
is chemically difficult to obtain unbranched nylon 3 by polymerization of β -alanine or by ring-opening of 2-azetidinone. To understand the mechanism of the CALB-mediated ring-opening polymerization and to learn from this reaction with respect to an enzymatic synthesis of other polyamides, we have investigated by computational simulation the molecular basis of the enzyme-catalyzed ring-opening reaction of β -lactam and the elongation of the monomer toward a poly(β -alanine).

In analogy to the generally accepted mechanisms of the CALB-catalyzed synthesis of esters, the polymerization of β -lactam should involve an initial acylation of Ser105 by a molecule of β -lactam, followed by amidation of the acylgroup by another β -lactam monomer and the reacylation of the serine to complete the chain elongation. A tetrahedral intermediate mimics the transition states both for formation and for collapse of the acyl intermediate.¹⁹ In view of the vast number of publications on the enzymatic synthesis of polyesters^{5,6,8,12,20} and of the higher nucleophilicity of amines as compared to alcohols, it is rather surprising that only a few CALB-catalyzed amide formations and even fewer polyamide syntheses have been reported so far.^{17,18} However, despite the ability of some β -lactam derivatives to

Received: October 7, 2010

Revised: January 20, 2011

Published: March 01, 2011

Scheme 1. Mechanistic Routes of Enzymatic β -Lactam Polymerization

inhibit serine hydrolases by formation of a stable acyl enzyme complex,²¹ a few ring-opening reactions of β -lactams catalyzed by CALB have been reported in addition to the ring-opening polymerization of Schwab et al.¹⁸ Adam et al.²² showed that α -methylene- β -lactam is transformed highly enantioselectively but very slowly to the open-chain β -amino acid. The α -methylene group in this case increases the ring strain, flattens the conformation of the ring, and withdraws electrons from the carbonyl group, thereby activating the β -lactam ring toward ring-opening. Park et al.²¹ demonstrated the ring-opening of 4-phenylazetidin-2-one and suggested that the reaction proceeds via an unusual substrate-assisted transition state in which a substrate alcohol bridges the catalytic histidine and the nitrogen of the β -lactam. The same group also reported a highly enantioselective ring-opening of unactivated alicyclic β -lactams by hydrolysis, which turned out to be considerably slower than the comparative alcoholysis.^{23,24}

However, not only the nucleophilicity but also the acid–base properties of reactants are to be considered. A deactivation of CALB by acids has recently been reported by Hollmann et al.,²⁵ who showed that organic acids exhibiting a pK_a value below 4.8 cause irreversible deactivation of CALB, but the corresponding esters do not show any inhibiting effects. A pK_a of 4.8 should, however, not be seen as a threshold value but, rather, as a point of orientation. There are acids exhibiting pK_a 4.8 that cause a strong inactivation of the enzyme but others do not have any effect on the enzyme. This depends on structural properties of the substrate. α - or β -substituents can cause a decrease in activity compared with the unsubstituted acid, whereas γ -substituents hardly influence the enzyme activity. Unfortunately, no information is provided for the pK_a range from 4.3 to 4.7 in this investigation. In this respect, it is of interest that adipic acid, having a pK_a value of 4.42,²⁶ does undergo the CALB-catalyzed polymerization with octanediol, yielding a polymer of high molecular weights.²⁷ β -Alanine with its pK_a of 3.6²⁸ is far below the critical value of 4.8 and can, therefore, be expected to inactivate the enzyme by protonation of His224. This corresponds to the experimental finding that β -alanine could not be used as starting material for the polymerization.^{18,29} It should, however, be kept in mind that all these pK_a values have been measured in water and could well differ in the special environment of a protein active site.

On the basis of these results, we set about the mechanistic explanation of the polymerization of β -lactam, of the inability of β -alanine to serve as the initiating or elongating monomer, and of the reason for the maximum chain length of only 18 monomer units. In our computational simulation approach, we started from the X-ray structure of CALB (PDB ID: 1LBS), which was

elucidated in 1995 by Uppenberg et al.³⁰ and which paved the way to an atomistic study of lipase-catalyzed reactions. CALB utilizes a catalytic triad of Ser105, His224, and Asp187, and in addition affords the amino acids Thr40 and Gly106, which form the oxyanion hole to stabilize the substrate in a transition state. The binding pocket of CALB can be divided into two subsides by the side chains of Ile189 and Ile285: the larger acyl side and the medium-sized alcohol side, named after the placement of different substrates in the binding site. An acyl chain will occupy the acyl side; nucleophiles such as alcohols or amines are hosted in the alcohol side.

Here, we describe the molecular basis of the ring-opening polymerization of unsubstituted β -lactam, starting from the initial formation of an acyl enzyme complex, which then enters a catalytic cycle for the chain elongation from which the growing chain eventually is released as poly(β -alanine).

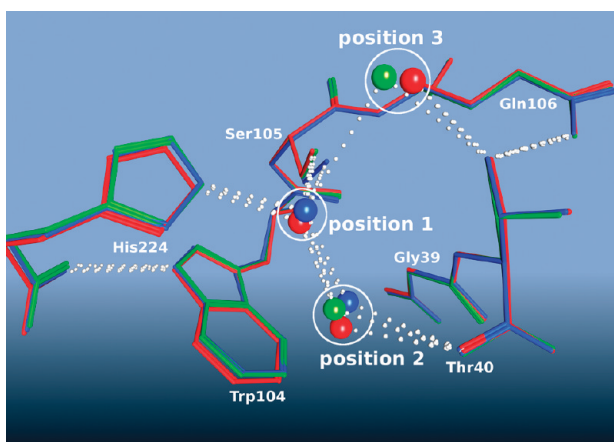
RESULTS AND DISCUSSION

Mechanistic explanations of lipase-catalyzed transesterification or amidation all follow the identical concept of an initial acylation of Ser105 by an appropriate carbonyl compound to yield an acylated intermediate, followed by liberation of the acyl group after a nucleophilic attack of an alcohol or an amine at the serine-bound carbonyl group, which gives the desired product. Both steps proceed via an intermediate structure that has a serine-bound carbon with tetrahedral geometry.

If one applies this mechanism to the formation of poly(β -alanine), the first step would involve an attack of Ser105 at the β -lactam (1) to yield the acyl enzyme intermediate (2) (Scheme 1). At this point, hydrolysis could occur if water is present, which would liberate β -alanine (3) that itself could serve as a building block in the polymerization process (path B). In this case, β -alanine has to be produced in reserve and stored inside the lipase or in the solvent, respectively. Accumulation of β -alanine in the organic solvent (e.g. toluene as used in the experiments of Schwab et al.¹⁸) is not possible because of its low solubility. However, a temporary storage of, for instance, one molecule of β -alanine inside the pocket would be conceivable in a position where it does not facilitate inactivation of CALB by the free acid.²⁵ With the findings of Schwab et al. that β -alanine is not a substrate for polyamide formation,²⁹ a plausible mechanism for the lipase-catalyzed formation of poly(β -alanine) in an organic solvent would involve β -lactam (1) as the initiating and elongating monomer, as shown in path A. Alternatively, β -lactam could enzymatically be hydrolyzed, stored outside the enzyme in the reaction medium, and could then diffuse back into the binding site to be used for chain elongation. This is represented by path B

Table 1. Calculated pKa Values of β -Alanine Oligomers

β -alanine units	1	2	>3
pKa (acid)	3.7 ± 0.4	4.0 ± 0.4	4.2 ± 0.4
pKa (base)	10.3 ± 0.4	9.4 ± 0.4	9.3 ± 0.4

**Figure 1.** Conserved crystallographic water positions inside the active site of native CALB (red, 1TCA.A; green, 1TCB.A; blue, 1TCB.B).

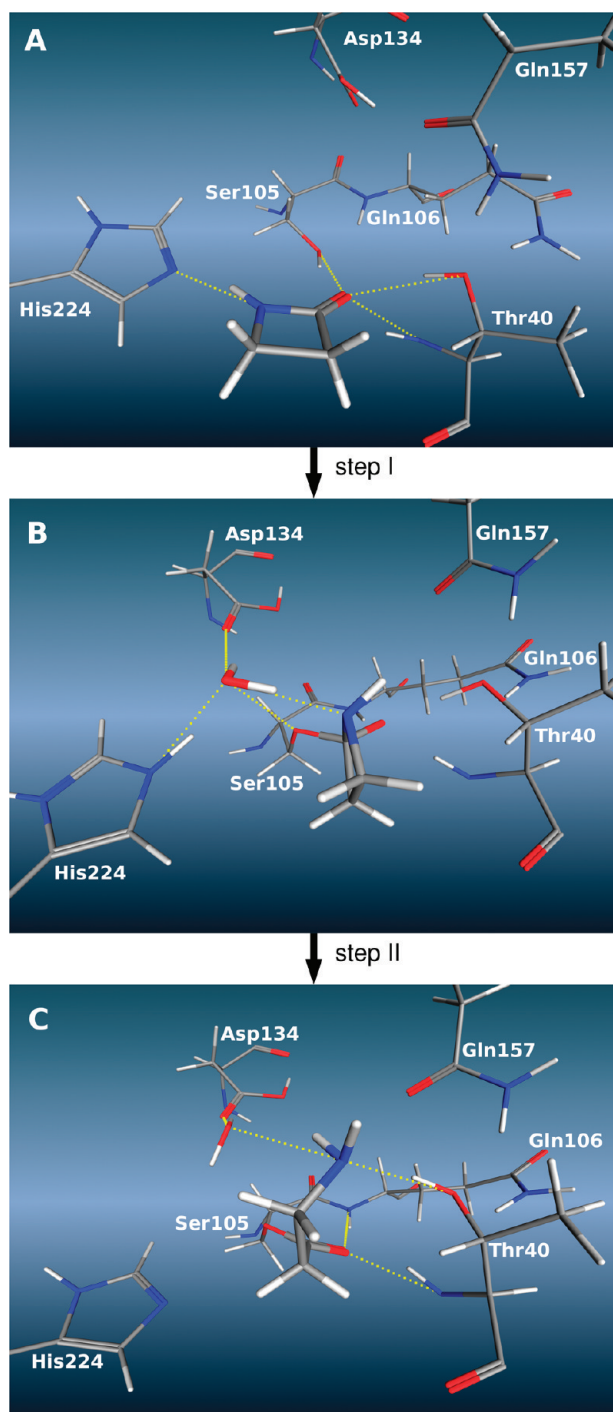
in Scheme 1 and corresponds to the commonly believed mechanism of enzymatic polymerization. In any case, this mechanism has to consider the lower nucleophilicity of the amide nitrogen of **1** as compared with the amine nitrogen of **3**.

In either instance, a serine-bound β -alanine dimer (**4**) is derived, which after further elongation steps could be released as poly(β -alanine) from the catalyst by hydrolysis. Although in case of path B, one molecule of water is temporarily used for each elongation step, path A could proceed without previous hydrolysis of all β -lactam monomers. However, keeping in mind that the reaction is carried out in an organic solvent using a dried preparation of Novozyme 435, one water molecule is necessary to liberate the final product from the enzyme, which has to be contributed from the water reservoir of the immobilized enzyme. In general, this is not a limitation of the reaction because CALB catalyzed polymerizations of lactones are well-known from the literature so that enough water seems to be available even with dried enzyme preparations.^{15,31,32}

In the synthesis of poly(β -alanine) from β -lactam (**1**) reported by Schwab et al.,¹⁸ the authors could also show that in contrast to pathway B of Scheme 1, β -alanine (**3**) is not a substrate for the lipase catalyzed synthesis of poly(β -alanine), a surprising result that was confirmed in a variety of different solvents to rule out a solvent dependency.²⁹ This result is in agreement with the findings of Hollmann et al.²⁵ who observed an inactivation of CALB by acids exhibiting a pKa below 4.8. The pKa of β -alanine (3.6)²⁸ is well below this critical value.

In addition, a possible mechanism has to take into account the acidity of the various β -alanine oligomers generated on the way to a poly(β -alanine). Because there is no experimental data available for β -alanine oligomers, we have predicted the corresponding pKa values using the ACDLab software³³ (Table 1) for comparison with the threshold value for inactivation reported by Hollmann.²⁵ The data were generated for an aqueous medium.

The experimental pKa value of β -alanine (3.6)²⁸ is reproduced with good accuracy by the calculation. Dimerization and trimerization of β -alanine result in an increase in the pKa value to 4.0

**Figure 2.** Interaction of β -lactam (**1**) with enzyme pocket (panel A). Attack of serine oxygen at the β -lactam carbonyl yields the first tetrahedral intermediate TI1 (step I). Covalent docking and QM/MM optimization of TI1 in the presence of water as proton shuttle (panel B). Ring-opening of TI1 gives a serine-bound β -amino acyl side-chain (acyl enzyme complex), which is located on the acyl side of the enzyme pocket (step II, panel C) as result of QM/MM geometry optimization.

and 4.2, respectively. Further chain elongation has no influence on the pKa. With the uncertainty on one hand of the calculated values and on the other hand of the possible lipase inactivation in the pKa range of 4.3–4.7, as discussed earlier, we cannot say much about the influence of the growing chain on the possible

Scheme 2. Catalytic Cycle of the *C. antarctica* Lipase B-Catalyzed β -Lactam Polymerization (for details, see the Results and Discussion)

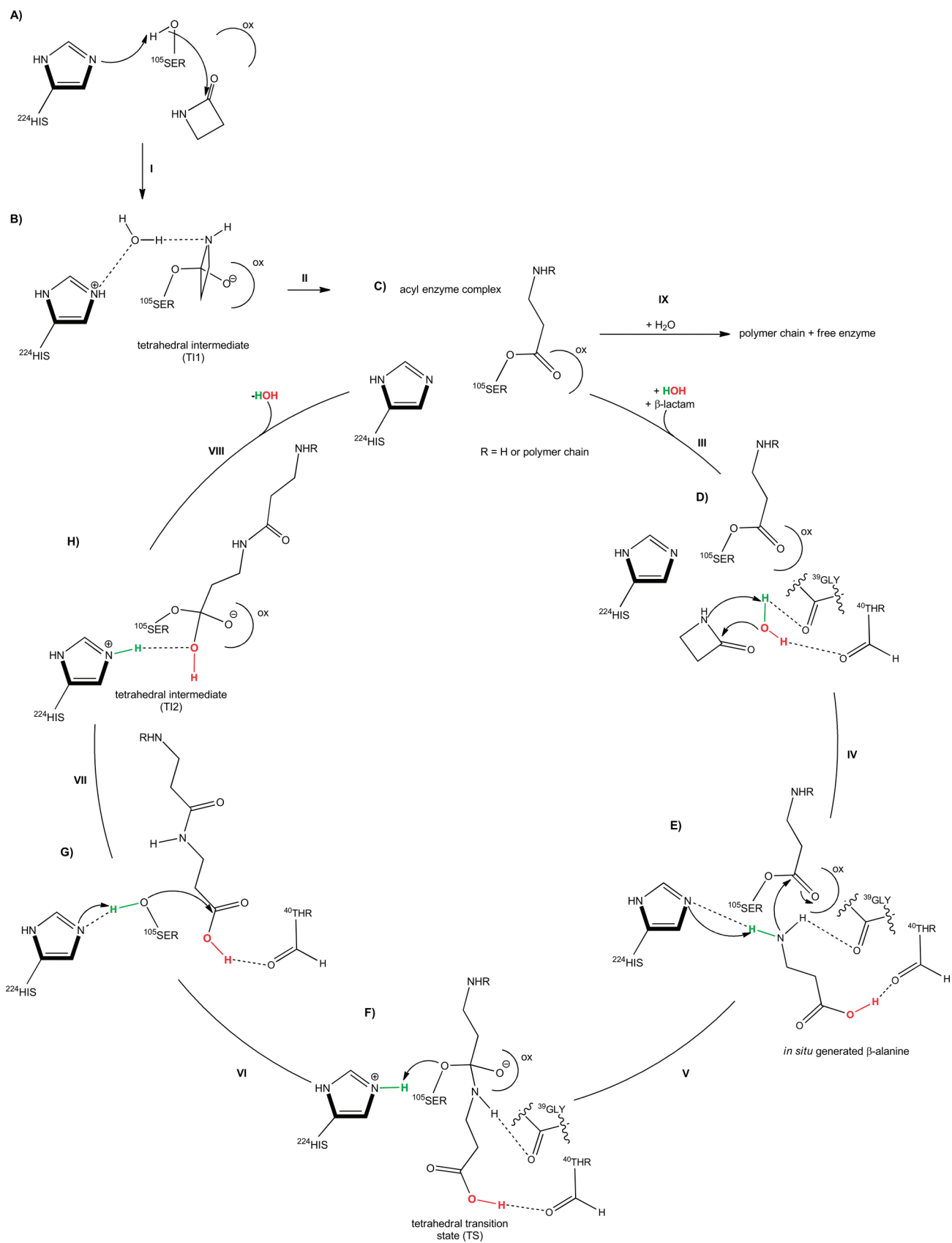


Table 2. Representative Conformations Collected from a MD Run of β -Lactam Inside CALB Active Site

MD run conformations	O(Ser105)–N(His224)		O(Ser105)–C=O(β -lactam)		resulting configuration of TI1
	distance (Å)	angle (deg)	distance (Å)	angle (deg)	
1	2.85	166.4	3.70	78.7	S
2	3.07	129.3	3.39	71.9	R

protonation of His224–N and, hence, on the activity of the enzyme. One can, however, expect that the probability of enzyme deactivation decreases with increasing length of the oligomer. In this respect, it is of interest that in contrast to a lipase-catalyzed polyester formation, β -lactam yields only short-length oligomers with a maximum of 18 and an average of 8 monomer units.^{18,29}

Bas et al. have described an effective procedure that allows calculation of the pK_a value of a carboxylic acid inside the enzyme pocket, depending on the acidity of neighboring protein groups.³⁴ Their web-based PROPKA procedure is an excellent tool to generate pK_a values of ligands inside the active site, which in our case, for instance, allows a comparison of the polyamide formation from β -lactam with a polyester formation from, for example, adipic acid and octanediol, the latter of which is known to proceed with high yields. If we assume β -alanine as the initial intermediate of β -lactam polymerization, the free acid, either β -alanine or adipic acid then, has to enter the active site with its carboxyl group directed down toward Ser105–O to acylate serine while the serine proton is transferred to the His224–N. If, however, the acid does not acylate the serine but instead protonates the histidine, the enzyme is inhibited because the carboxylate anion could not be attacked by serine anymore, and no acceptor is available to take up the serine proton.

We have therefore compared the interaction of β -alanine and adipic acid with the catalytic site of the binding pocket by positioning these acids manually inside the pocket with their acidic protons identically pointing toward His224–N, followed by a refinement of the structures by a series of energy minimizations. A pK_a calculation of these acids inside the free enzyme then yields 2.46 for β -alanine (His224: 10.03) and 3.10 for adipic acid (His224: 8.68).

Similarly, in the elongation step of the polymerization process, an acid could enter the active site of an acylated enzyme rather than a nucleophile, as necessary. Again, His224 could be protonated in this case, which would terminate the polymerization. We have, therefore, also compared the pK_a values of β -alanine and adipic acid inside the active site of a serine-acylated CALB (acylation by the respective acid). Again, both acids were analogously positioned in front of His224, and the complexes were energetically minimized as described for the free enzyme. The pK_a calculations of these complexes yield a value of 4.37 for β -alanine (His224: 8.55) and 5.50 for adipic acid (His224: 9.60). Even though the particular conformation of the acids presumably does not resemble global minima, it is striking to realize that β -alanine is the much stronger acid inside the active site than adipic acid.

Modeling of the Ring-Opening Polymerization of β -Lactam. We have simulated the CALB-catalyzed β -lactam polymerization of β -lactam using a combination of a force-field-based docking procedure and a comprehensive QM/MM theoretical method to describe the reaction path in detail in which the interactions in the QM region were modeled with great accuracy at the DFT/B3LYP level of theory and the surrounding protein and solvent water were considered in the MM region using a faster

molecular mechanical treatment. The results of these calculations are combined in a catalytic cycle (Scheme 2) that consists of two starting steps (I and II) leading to an acyl enzyme complex, six steps for the chain elongation (III–VIII) utilizing an in situ-generated β -alanine and that is completed by the release of the polymer (IX). These nine steps are discussed in detail in the following paragraphs.

Since the experimental studies were conducted in toluene and the QM/MM theoretical investigations of the reaction mechanism were performed in a water box, COSMO (conductor-like screening model) calculations using toluene dielectric were additionally carried out for the first three steps of the catalytic cycle to provide additional support of our results. We can show that using the implicit solvent model of toluene around the quantum mechanical region of the previous QM/MM calculations results in exactly the same pathway as described for water in the following paragraph, with only a 2 kcal/mol lower energy.

Step I. Docking studies of β -lactam into the active side of CALB show that the monomer is positioned in an energetically favored position within the so-called alcohol side of the pocket (Figure 2A). This pose is stabilized by strong hydrogen bonds to Ser105, Thr40 (OH and NH group) and His224 (2.52 Å, 3.02 Å, 2.72 Å and 2.71 Å respectively). It should be noted, however, that a predominant binding mode resulting from docking does not always resemble the catalytically productive binding pose, but rather might first have to overcome a further energy barrier, as has been reported by Veld et al.³⁵ for binding modes of cisoid and transoid lactones. A 1 ns MD run proves that the β -lactam resides permanently close to Ser105 so that an attack of Ser105–O at the carbonyl carbon of β -lactam seems very likely. The resulting tetrahedral intermediate TI1 (Figure 2B) can have S or R configuration, depending on the position of the former lactam carbonyl carbon during the attack of Ser105. In the above-mentioned MD run, conformations leading to both enantiomers can be observed. Table 2 displays representative data for two different conformations collected during the MD run of β -lactam inside CALB active side.

Step II. The attack of Ser105–O on the β -lactam carbonyl results in a first tetrahedral intermediate TI1, which again can have R or S configuration at the former lactam carbonyl, and cis or trans configuration of the NH proton with respect to the negatively charged oxygen. Ring-opening of this first tetrahedral intermediate requires a proton transfer from His224–N to the ring nitrogen of the former β -lactam. This affords a cis configuration of the NH proton and a suitable distance and angle between the ring nitrogen and His224–N. Structural optimization of the S and R enantiomers of TI1 both reveals a cis configuration of the NH proton. However, a rapid inversion of the former lactam ring can be expected at room temperature, and both configurations are equilibrated. Docking and subsequent QM/MM optimization on one hand of the S enantiomer of TI1 demonstrate that His224 is directed toward Ser105–O so that no reaction with the former β -lactam monomer can take place, which instead leads to a release of β -lactam from the binding site

Table 3. Hydrogen Bonds between (a) the Tetrahedral Intermediate TI1 and the Oxyanion Hole and (b) between the Catalytical Water Molecule and the Surrounding Protein after QM/MM Optimization

	(a) TI1–Oxyanion Hole O(TI1)–NH(Gln106)	O(TI1)–OH(Thr40)	O(TI1)–NH(Thr40)
distance (Å)	2.84	2.71	2.71
angle (deg)	164.9	176.7	176.0
		(b) H ₂ O O(H ₂ O)–NH(TI1)	O(H ₂ O)–NH(His224) O(H ₂ O)–O(Asp134)
distance (Å)	2.67	2.55	3.12
angle (deg)	168.2	162.5	161.4

Table 4. Interaction of the Acyl Enzyme Complex (aec) with the Oxyanion Hole and the Catalytic Water Molecule after (a) Docking and (b) QM/MM Optimization

(a) Acyl Enzyme Complex–Oxyanion Hole (Docking Result)			
	O(aec)– NH(Gln106)	O(aec)– OH(Thr40)	O(aec)– NH(Thr40)
distance	3.17	2.86	2.62
(Å)			
angle (deg)	133.0	163.5	161.7
(b) Acyl Enzyme Complex–Catalytic Water Molecule (QM/MM Optimization)			
	O(aec)– NH(Gln106)	O(aec)– OH(Thr40)	O(aec)– NH(Thr40)
distance	2.77	3.37 ^a	2.70
(Å)			
angle (deg)	165.0	94.5 ^a	155.2
	NH ₂ (aec)– OH(Thr40)	NH ₂ (aec)– H ₂ O	H ₂ O– O(Asp134)
distance (Å)	2.74	2.91	2.76
angle (deg)	163.3	136.6	166.9

^a No hydrogen bonding.

(data not shown). If, on the other hand, the *R* enantiomer is treated this way, the simulation yields a structure in which the distance between His224–N and the NH group of the former lactam ring is too large for a proton transfer; that is, the necessary ring-opening cannot occur. However, we can show that a water-mediated proton transfer could take place, as already described for other CALB-catalyzed reactions, in which alcohol or water serves as a proton shuttle.^{21,36,37} The crystal structure of native CALB (PDB ID: 1TCA and 1TCB)³⁸ features several crystallographic water molecules, which indicates positions favorably occupied by water. One of these positions is in front of His224, exhibiting a hydrogen bond to His224–N (position 1, Figure 1). In addition, another conserved water is found near Thr40 with correct hydrogen bonding distance to the Thr40 backbone carbonyl (position 2, Figure 1). The third conserved water position in the binding site is located in hydrogen bonding distance to the Thr40 hydroxy group, slightly above the oxyanion hole (position 3, Figure 1). These water positions are used in docking studies of structures B and D (Scheme 2) and in all subsequent QM/MM studies of the catalysis cycle.

We have therefore manually added a water molecule to the *R* and *S* enantiomer of the tetrahedral intermediate TI1 at a

position in front of His224–N, followed by energy minimization of the system. In case of the *R* enantiomer, this water molecule stays in front of His224–N during covalent docking of β -lactam to Ser105 and subsequent energy minimization and QM/MM optimization. The water molecule is stabilized efficiently by hydrogen bonding to the former lactam nitrogen, His224–N and Asp134–O. The negatively charged oxygen is stabilized by the oxyanion hole, as depicted in Figure 2B. Table 3 shows data of hydrogen bonds between the *R* enantiomer of TI1 and the water molecule used for the proton shuttle. In contrast, the *S* enantiomer lacks such a stabilization of the water molecule, which rather migrates toward the acyl side of the pocket during energy minimization instead of staying between His224–N and the ring nitrogen of the former lactam ring. From these results, we conclude that the *R* conformation of TI1 is essential for the further progress of the reaction.

Ring-opening of the *R* enantiomer of TI1 is mediated by proton transfer from His224 to TI1 via the above-mentioned water molecule used as proton shuttle. We have simulated this proton transfer by QM/MM calculation applying the “spring method” of NWChem.^{39,40} For this procedure, a spring was set between the water proton and the ring nitrogen of the β -lactam, followed by a QM/MM optimization.

This method yields a structure in which a proton is transferred from the catalytic water molecule in front of His224 to the ring nitrogen of the former lactam while the water oxygen takes up the His224 proton. As a consequence, the lactam ring is opened and an acyl enzyme complex is formed. The acyl chain moves to the acyl side of the pocket while the alcohol side is emptied (Figure 2C). An almost identical positioning of the acyl chain can be found by covalent docking of the acyl enzyme complex (Figure 3C). Table 4 shows interaction data for hydrogen bonding of the acyl enzyme complex in the QM/MM and the docking experiment, respectively. QM/MM calculation reveals an additional stabilization by hydrogen bonding of the acyl enzyme complex to the water molecule used as proton shuttle. One hydrogen bond of the carbonyl carbon of the acyl enzyme complex to Thr40–NH is lost in favor of a hydrogen bond to the amino group of the acyl enzyme complex (Table 4). The water molecule that was used as proton shuttle is now located between the amino group of the acyl enzyme complex and Asp134. Because another water molecule is later needed in the alcohol side of the binding pocket for chain elongation, water has to move back or be replaced by another one from the enzyme’s water reservoir.

Step III. As already discussed, elongation of the acyl enzyme complex can proceed only via attack of a β -lactam monomer rather than by a β -alanine at the acyl enzyme complex. However,

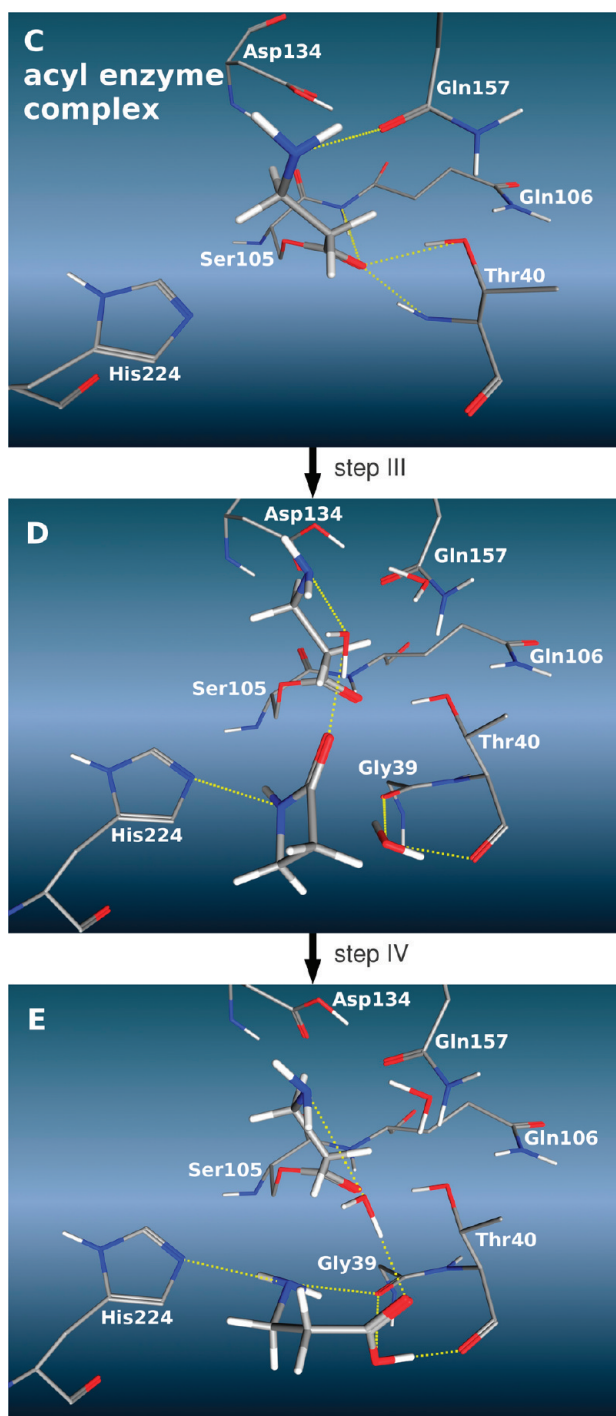


Figure 3. Covalent docking of the serine-bound β -amino acyl side chain results in a positioning in the acyl side of the pocket (panel C) similar to the conformation gained in QM/MM optimization (Figure 2C). Docking of a second β -lactam monomer into the acylated enzyme in the presence of a crystallographic water molecule and subsequent QM/MM studies (step III, panel D) result in activation of β -lactam by attack of the hydroxy group of this water molecule, yielding an activated monomer (step IV, panel E).

the low electron density of the β -lactam nitrogen prohibits a direct attack at the Ser105-bound carbonyl group. Instead, the β -lactam monomer has first to be activated by diminishing the double bond character of the amide bond. This can be achieved

by a nucleophilic attack of a water molecule at the lactam carbonyl group. As described earlier, several crystallographic water molecules are present in the alcohol side of the enzyme. Two of those thermodynamically preferred positions are in front of His224 (position 1, Figure 1) and in front of Thr40 (position 2, Figure 2), respectively. The water molecule in the hydrogen bonding vicinity to His224-N has already been used as proton shuttle in step II.

Docking studies of β -lactam into the acylated enzyme in the presence of a water molecule in hydrogen bonding distance to Thr40 followed by QM/MM optimization yield the structure depicted in Figure 3D. β -Lactam in this structure is stabilized by strong hydrogen bonds to a further solvent molecule in hydrogen bonding distance (2.77 \AA , 163.6°) and a weak interaction with His224-N (3.36 \AA , 144.9°), whereas the catalytic water molecule shows two strong hydrogen bonds to the carbonyl groups of Gly39 (2.62 \AA , 155.8°) and Thr40 (2.60 \AA , 161.0°). The acyl enzyme complex is stabilized by two of the three hydrogen bonds representing the oxyanion hole (Table 5). The hydrogen bond to Thr40-NH is lost in favor of a reorientation of the peptide bond, which enables a stabilization of the water molecule by Gly39-CO. In the resulting structure, the distance between the water oxygen and the carbonyl carbon of β -lactam is ideal for an *in situ* ring-opening of the β -lactam (2.90 \AA , 109.4°), which was simulated in a QM/MM calculation by first applying a spring between the water oxygen and the lactam carbonyl carbon, followed by a spring between the water proton and the lactam nitrogen.

This attack of water on β -lactam yields an *in situ*-generated β -alanine that is ready to attack the acyl enzyme complex. The water molecule utilized for the ring-opening is, however, not consumed, but rather, is released again in step VIII, that is, made available for the next activation step in the following cycle. This catalytic water molecule could possibly be identical to the one used as proton shuttle in step II because both water positions are rather close to each other. It should, however, be kept in mind that a water molecule close to His224 or Thr40 is also close to Ser105 and could equally well cleave the acyl enzyme complex, which would result in the release of oligo(β -alanine). Chain elongation is, therefore, always in competition with chain termination, which explains the low molecular weight of the material obtained by Schwab et al.²⁹

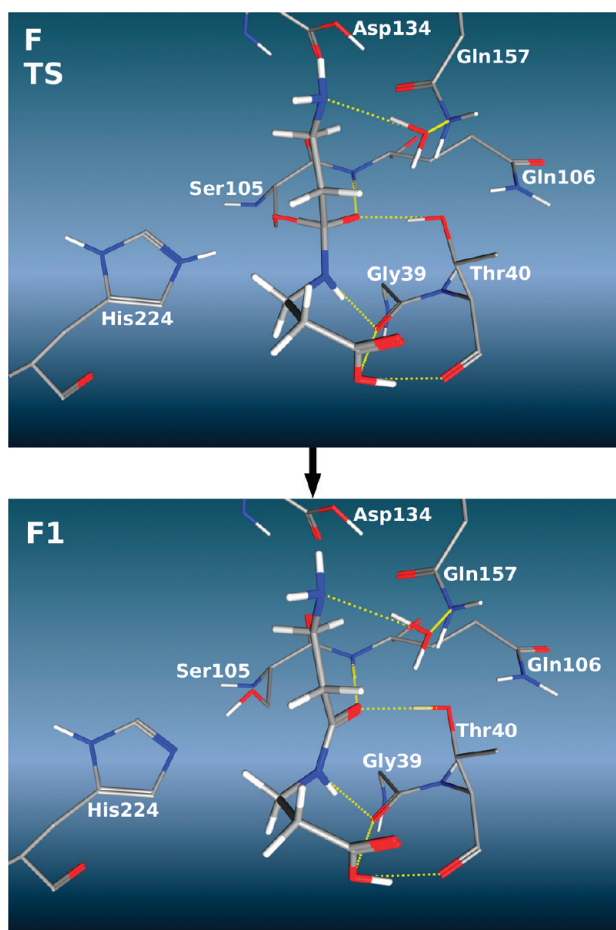
Step IV. Step IV of our simulation describes the activation of the β -lactam necessary for the desired nucleophilic attack at the serine bound carbonyl. Starting from the structure depicted in Figure 3D, the activation was achieved by a QM/MM simulation of the attack of a catalytic water molecule at the β -lactam carbonyl. In a two-step procedure, a first spring was set between the water OH group and the carbonyl carbon, followed by a second spring between the water proton and the ring nitrogen of the former lactam. A subsequent QM/MM optimization yields an *in situ*-generated β -alanine, which is stabilized by hydrogen bonding to Thr40-CO (2.55 \AA , 176.3°), Gly39-CO (3.00 \AA , 161.2°), a conserved water molecule (2.88 \AA , 169.6°), and a weak interaction with His224-N (3.27 \AA , 156.2°) (Figure 3E). The acidic proton of β -alanine is directed toward the backbone carbonyl group, which prevents protonation of His224 and inactivation of the enzyme. Calculation of the acid pK_a in this conformation with the PROPKA web interface yields a value of 8.54 for the acid group (His224: 5.08), a rather high value for an acid. The acyl enzyme complex remains stabilized by two of the three hydrogen bonds of the oxyanion hole (Table 6), whereas

Table 5. Characterization of the Interaction of the Acyl Enzyme Complex (aec) with the Oxyanion Hole in Figure 3D

	acyl enzyme complex–oxyanion hole		
	O(aec)–NH(Gln106)	O(aec)–OH(Thr40)	O(aec)–NH(Thr40)
distance (Å)	2.77	2.60	3.74
angle (deg)	158.2	166.4	49.1

Table 6. Interaction of Acyl Enzyme Complex (aec) with the Oxyanion Hole As Shown in the Structure of Figure 3E as a Result of Docking and QM/MM Simulation

	acyl enzyme complex–oxyanion hole		
	O(aec)–NH(Gln106)	O(aec)–OH(Thr40)	O(aec)–NH(Thr40)
distance (Å)	2.77	2.63	3.52
angle (deg)	158.9	169.8	55.8

**Figure 4.** Dimeric transition state derived from attack of the in situ-generated β -alanine at the serine-bound carbonyl C (panel F) which results in a release of a dimeric β -alanine (panel F1).

the hydrogen bond to Thr40–NH is abolished to allow a stabilization of the β -alanine monomer by Gly39–CO. The in situ-formed β -alanine is an adequate monomer for chain elongation because the electron density of the amino group is significantly increased compared with β -lactam and the orientation of β -alanine is suitable for an attack at the carbonyl carbon of the acyl enzyme complex (3.28 Å, 95.0°). With this in situ generation of a β -alanine monomer in front of Thr40, chain

elongation can instantly take place without reorientation of β -alanine, which potentially would lead to protonation of His224.

Step V. Electron density and distance of the amino group of the in situ-generated β -alanine to the serine carbonyl (3.28 Å, 95.0°) are sufficient for a nucleophilic attack. We have simulated this step by applying a spring between the alanine nitrogen and the carbonyl carbon of the acyl enzyme complex, which yields the protonated tetrahedral transition state TS. Afterward, applying a second spring between the now positively charged nitrogen of the former β -alanine and His224–N results in the unstable dimeric TS, as depicted in Figure 4F. Table 7 describes the structural data of TS derived from QM/MM calculations. The acid group of TS is still stabilized by a quite short hydrogen bond to Thr40, whereas the NH group is directed toward Gly39. Furthermore, the negatively charged oxygen of TS is comfortably nested in the oxyanion hole by two hydrogen bonds, and the negative charge is compensated by the positive nitrogen charge of His224–N. This transition state, however, is rather unstable, since further QM/MM optimization after removing the constraints yields the release of the generated dimer (Figure 4F1).

Step VI. Further optimization of the dimeric tetrahedral transition state TS results in a release of the dimer by proton transfer from His224 nitrogen to the Ser105 oxygen. The detached dimer (Figure 4F1) remains close to its original position during a subsequent QM/MM optimization, featuring hydrogen bonds similar to TS (Table 8). Rebinding of the dimer with its terminal carboxyl group to Ser105 requires migration toward the acyl side of the pocket, which directs the terminal amino group toward the exit of the binding pocket. It is important at this point that the dimer does not have to leave the binding site but, rather, traverses the alcohol side of the binding pocket to properly position the molecule for the next elongation step.

We have employed docking techniques to generate a potential structure that after this molecular translation would allow continuation of the chain elongation. These docking studies of the dimer with subsequent QM/MM optimization indeed reveal such a structure that is properly positioned for rebinding of the carboxyl terminus (Figure 5G). The acidic proton of the dimer in this structure is still within hydrogen bonding distance to Thr40–O (2.60 Å, 150.2°), which suggests that this hydrogen bond remains intact during the entire migration process of the chain, and thus, a protonation of His224 is prevented. The pK_a calculations of this dimer conformation yield a value of 6.35 for

Table 7. Interaction of Dimeric Tetrahedral Transition State TS with Oxyanion Hole and Surrounding Protein Resulting from QM/MM Calculations

	O(TI2)–NH(Gln106)	O(TI2)–OH(Thr40)	O(TI2)–NH(Thr40)	OH(TI2)–O(Thr40)	NH(TI2)–O(Gly39)
distance (Å)	2.70	2.58	3.44	2.55	2.78
angle (deg)	173.2	171.9	66.1	168.0	169.2

Table 8. Interaction of the Released Dimer (F1) with Surrounding Protein As Resulting from Docking and QM/MM Calculations

	O(dimer)–NH(Gln106)	O(dimer)–OH(Thr40)	O(dimer)–NH(Thr40)	OH(dimer)–O(Thr40)	NH(dimer)–O(Gly39)
distance (Å)	2.96	2.57	3.40	2.55	2.71
angle (deg)	169.8	163.7	61.6	166.3	163.3

the carboxyl group (His224: 6.43). Further stabilization of the dimer is gained by hydrogen bonding of the terminal carboxyl oxygen to Thr40–NH (2.87 Å, 124.9°) and of the peptide oxygen to Thr40–OH (2.82 Å, 166.7°).

Steps VII and VIII. Step VII simulates rebinding of the dimer at the carboxyl terminus by attack of Ser105. During the migration of the released dimer (see Figure 4F1 and 5G) through the binding pocket, the carboxyl terminus stays positioned near Ser105–O, still featuring a hydrogen bond of the OH group to Thr40. The terminal carbonyl carbon is already hydrogen-bonded to the oxyanion hole (Thr40–NH) and is pulled into the oxyanion hole completely on rebinding of the dimer to Ser105. The distance between the carboxyl carbon of the dimer and Ser105–O (3.6 Å, 64.4°) is not ideal for an attack of Ser105; however, this attack can be simulated by applying the spring method of NWChem. A spring is set between Ser105–O and the carboxyl carbon of the dimer, which results in the second tetrahedral intermediate TI2 (Figure 5H). Alternatively, the dimer was first moved closer to Ser105 by applying a constraint of 2.86 Å between Ser105–O and the terminal carboxyl carbon of the dimer. After release of the constraint, the dimer stays in this position during the subsequent QM/MM optimization and can be rebound to Ser105 by application a spring of 1.3 Å (data not shown), which results in a structure identical to the one derived by direct rebinding. At this stage, the negatively charged oxygen of TI2 is stabilized by the oxyanion hole, the terminal amino group exhibits a hydrogen bond to the backbone carbonyl of Gln157, and the hydroxy group of TI2 shows hydrogen bonding to His224–NH (see Table 9).

The hydrogen bond between the hydroxy group of the dimer and His224–NH suggests a protonation of the OH group, which would initiate the release of water and the reformation of a serine-bound carbonyl group. This process can be simulated by a QM/MM calculation applying a spring between the hydroxyl group of TI2 and the His224 proton, resulting in a water molecule and an elongated acyl enzyme complex equivalent to the elongated structure C in Scheme 2 (Figure 5C1). The water molecule liberated during this step can be used again as a catalytic water molecule in step IV for activation of the next β-lactam monomer. Hence, the elongation process is neutral with respect to the water reservoir of the enzyme.

At this point, the catalysis cycle is completed, and the elongated acyl enzyme complex can be either extended further by the next activated monomer via step III or released by attack of a water molecule at the serine-bound carbonyl carbon (step IX). In the case of a release, the oligomer could either potentially protonate His224–N and thereby inactivate the enzyme or it could diffuse out of the binding side into the solvent with a given

probability to come back with correct orientation to continue the process of chain elongation.

CONCLUSION

Despite the fact that enzyme-catalyzed ring-opening polymerizations of lactones have been shown to yield high-molecular-weight polyesters,¹² the analogous approach to polyamides of similar degree of polymerization has as yet not been successful. The only appreciable result so far is an oligomerization of unsubstituted β-lactam by *C. antarctica* lipase B, recently published by Schwab et al.^{18,29} The authors show that the CALB-catalyzed polymerization only yields a product of low molecular weight with a maximum of 18 and an average of 8 monomer units. To understand this phenomenon, we have studied the reaction sequence involved on a molecular level using various computational methods, such as docking approaches, molecular dynamic simulations, and QM/MM methods based on high-level DFT calculations.

As a result, we propose a reaction sequence (Scheme 3) that starts with an initial positioning of a β-lactam in the active site (A) and the nucleophilic attack of Ser105 at this monomer to form a first tetrahedral intermediate TI1 (B). Ring-opening of TI1 takes place via a catalytic water molecule, which is used as proton shuttle that delivers a proton from His224 nitrogen to the ring nitrogen of the former β-lactam. The resulting acyl enzyme complex (C) then enters a catalytic cycle of six steps (C to H) that is completed with the formation of a homologue of the initial acyl enzyme complex (C), just extended by one monomer unit. From this complex, either the reaction can proceed by further elongation or the acyl chain can be cleaved from Ser105 by water to yield a polymer that eventually moves out of the enzyme.

Although the chain termination consumes a molecule of water that has to be supplied by the enzyme or the polyacrylic resin used for immobilization, there is also a water molecule necessary in the catalytic cycle for the chain elongation to proceed. This catalytic water molecule has to be located near His224 and Thr40; that is, at positions known to be conserved positions for crystallographic water molecules in the crystal structure of native CALB.³⁸ In our proposed reaction sequence, we initially make use of the water molecule near His224 as proton shuttle to form the first acyl enzyme complex TI1. Because this water is not consumed, it can be used as a catalytic water molecule. It is utilized to activate every single monomer during the chain elongation process (step IV), but it is always released again in the final step of the catalytic cycle (step VIII).

Although this water molecule is vital for the catalysis to take place, it is at the same time also responsible for the low-molecular-weight polymer achievable by CALB-catalyzed polymerization of

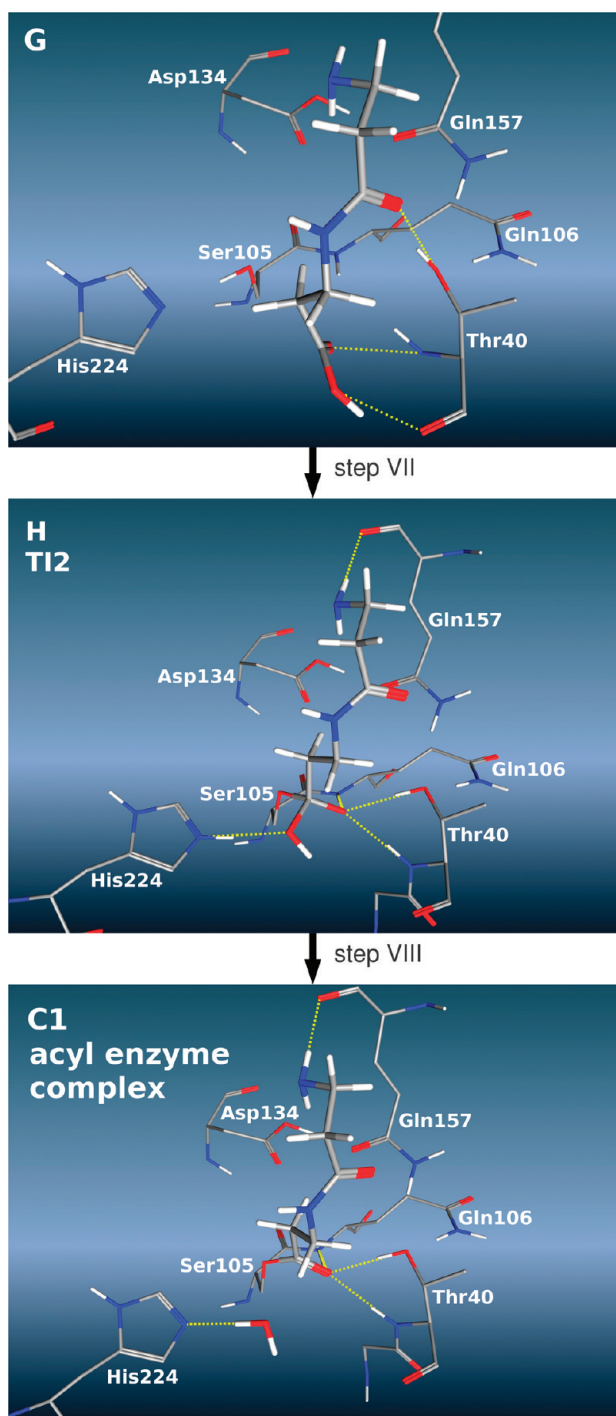


Figure 5. After the first elongation step, the generated dimer is detached from serine (panel G). After migration toward the acyl side exit, it can rebind to serine with the newly generated carboxyl terminus, yielding the tetrahedral intermediate TI2 (panel H). Protonation of the terminal OH group results in loss of water, leading to the structure C1, which resembles structure C extended by one monomer unit (panel C1).

β -lactam. A water molecule in front of His224 is always also close to Ser105 and will, therefore, constantly cause a competition between chain elongation and chain termination in step III of the catalytic cycle. If chain elongation wins at this point (D), the water molecule is used to build an in situ-generated β -alanine (E)

in step IV. Activation of the monomer is necessary because of the low electron density of the β -lactam and to abolish the partial double bond character of the amide bond that would prevent a nucleophilic attack at the acyl enzyme complex in step V. Our studies show that the in situ-generated β -alanine is anchored at Thr40 with its carboxyl group, which prevents a protonation of His224 and, therefore, inactivation of the enzyme. This anchor remains during step VI and is not detached until formation of the tetrahedral intermediate TI2. The in situ-generated β -alanine (E) is well positioned to attack the acyl enzyme complex (step V) while a proton is transferred from the β -alanine amino group to His224-N, yielding the dimeric transition state TS (F). QM/MM optimization of this structure shows the release of a β -alanine dimer by proton transfer from His224-NH to Ser105-O. The acidic proton of the released dimer remains attached to Thr40 by hydrogen bonding while the chain unfolds and migrates toward the acyl side exit of the pocket. Docking studies and subsequent QM/MM calculations reveal such a conformation (G), which allows rebinding of the dimer by attack of Ser105-O at the terminal carboxyl carbon (step VII), resulting in the tetrahedral intermediate TI2 (H) exhibits a hydrogen bond between the remaining hydroxy group and His224-NH, which results in separation of the catalytic water molecule (step VIII) and formation of an elongated acyl–enzyme complex (C).

It should be noted, however, that without calculations of the reaction energy profile of the complete catalytic cycle, the energetic picture of the enzymatic polymerization of β -lactam is still incomplete. Even though the presented results are to our knowledge the first investigation of such an enzymatic reaction on an atomistic level, our QM/MM simulation can only qualitatively support the proposed mechanism, and it rather awaits a true energetic profile to fully understand the reaction. Investigations along these lines are presently in progress in our group.

The described *C. antarctica* lipase B-catalyzed polymerization of β -lactam is limited by the requirement of one water molecule per liberated polymer chain, which has to be provided from residual water in the enzyme. Therefore, Novozyme 435, even though it is for obvious reasons used in a dry solvent, has to provide enough water in positions suitable to replace a water molecule consumed in chain dissociation from Ser105. Without this water in place, neither could the β -lactam monomer be activated nor could the elongation proceed, and finally, the polymer could not be released from the enzyme, and hence, this particular molecule of enzyme would be blocked from further activity.

However, the consumption of a water molecule per liberated chain seems not to be the limiting condition in the polymerization process. The CALB catalyzed polymerization, for instance, of ϵ -caprolactone similarly requires one molecule of water per polymer chain and has been shown to yield a high-molecular-weight material.¹¹ Obviously, the water reservoir even in dried enzyme preparations is sufficient not to hinder polymerization. In this respect, it is of interest that Schwab et al. could show that the CALB-catalyzed ring-opening polymerization of β -lactam shows an even lower molecular weight average than 8 when Novozyme preparations with too high or too low a water content is used, respectively.²⁹ Obviously, as long as a water molecule is present in the vicinity of His224 and Thr40, the major concern is the competition between activation of a β -lactam monomer (step III) and liberation of the oligomer (step IX), and hence, the probability of a premature chain termination is quite high.

Table 9. Stabilization of Terminal Bound Tetrahedral Intermediate TI2 As a Result of QM/MM Geometry Optimization

	interactions of tetrahedral intermediate TI2				
	O(TI2)–NH(Gln106)	O(TI2)–OH(Thr40)	O(TI2)–NH(Thr40)	NH ₂ (TI2)–CO(Gln157)	OH(TI2)–NH(His224)
distance (Å)	2.89	2.92	2.90	2.96	2.89
angle (deg)	171.9	173.8	174.1	171.1	168.3

Two steps of the catalytic cycle contain free carboxylic acids (E and G), in which the acidic proton is anchored by hydrogen bonding to Thr40 and both acids undergo further reaction directly from this position. The pK_a calculations show that these acid conformations are uncritical for protonation of the active site histidine His224. Nevertheless, if the in situ-generated β -alanine (E) or the released oligomer (G) are not instantaneously used for chain elongation, structural flexibility or migration of these acids could potentially inhibit further enzyme activity by protonation of His224.

With respect to the CALB-catalyzed ring-opening polymerization of β -lactam, we can conclude that a catalytic water is necessary as part of the catalytic cycle. This water molecule, however, could possibly also open the β -lactam ring, followed by diffusion of the generated β -alanine out of the binding site into the solution. Small amounts of β -alanine are, indeed, detectable in the solution,¹⁸ but because the solubility of β -alanine in the reaction medium (toluene) is low (10^{-5} mol L⁻¹), a detrimental effect of the β -alanine will be limited. In addition, the catalytic water molecule is also responsible for the competition of chain elongation and termination and, hence, for the low-molecular-weight material. Furthermore, the yield obtained in the polymerizations and the achieved average degree of polymerization of the obtained polymer is certainly also limited by its solubility in the reaction medium.

The CALB-catalyzed polymerization of lactones has not yet been computationally investigated. It can be expected that the lactone polymerization does not require a catalytic water molecule because the electron density of a lactone oxygen is higher than at the lactam nitrogen, and activation of the monomer is probably not required. DFT studies of El Firdoussi et al. give an idea of the very different electronic structures and properties of lactones and lactams.⁴¹ Assuming a mechanism for a ring-opening polymerization for lactones as we here postulate for β -lactam, the lactone polymerization should not be terminated as much as the lactam polymerization and, therefore, should yield a polymer of appreciable length. When there is no water present in the active site, there is no permanent competition between chain elongation and termination. In this respect, the enzymatic ring-opening polyamide formation differs from the corresponding polyester synthesis because chain elongation using β -lactam always requires one molecule of water. However, eventually, one water molecule is, of course, necessary in either case to terminate the polymerization and to liberate the polymer. That is, only when a water molecule occasionally is present in a suitable location of the active site will there be a temporary competition. In addition, in the case, for instance, of a CALB-catalyzed ring-opening polymerization of ϵ -caprolactone, 6-hydroxyhexanoic acid can potentially be released, which exhibits a pK_a of 4.75³³ and, therefore, should not show inactivation of CALB. To confirm the experimentally different results of CALB-catalyzed polyester and polyamide formation, the molecular mechanism, for instance, of the ring-opening polymerization of ϵ -caprolactone is of interest, and a computational study of the corresponding reaction sequence is, hence, in progress in our laboratory.

EXPERIMENTAL SECTION

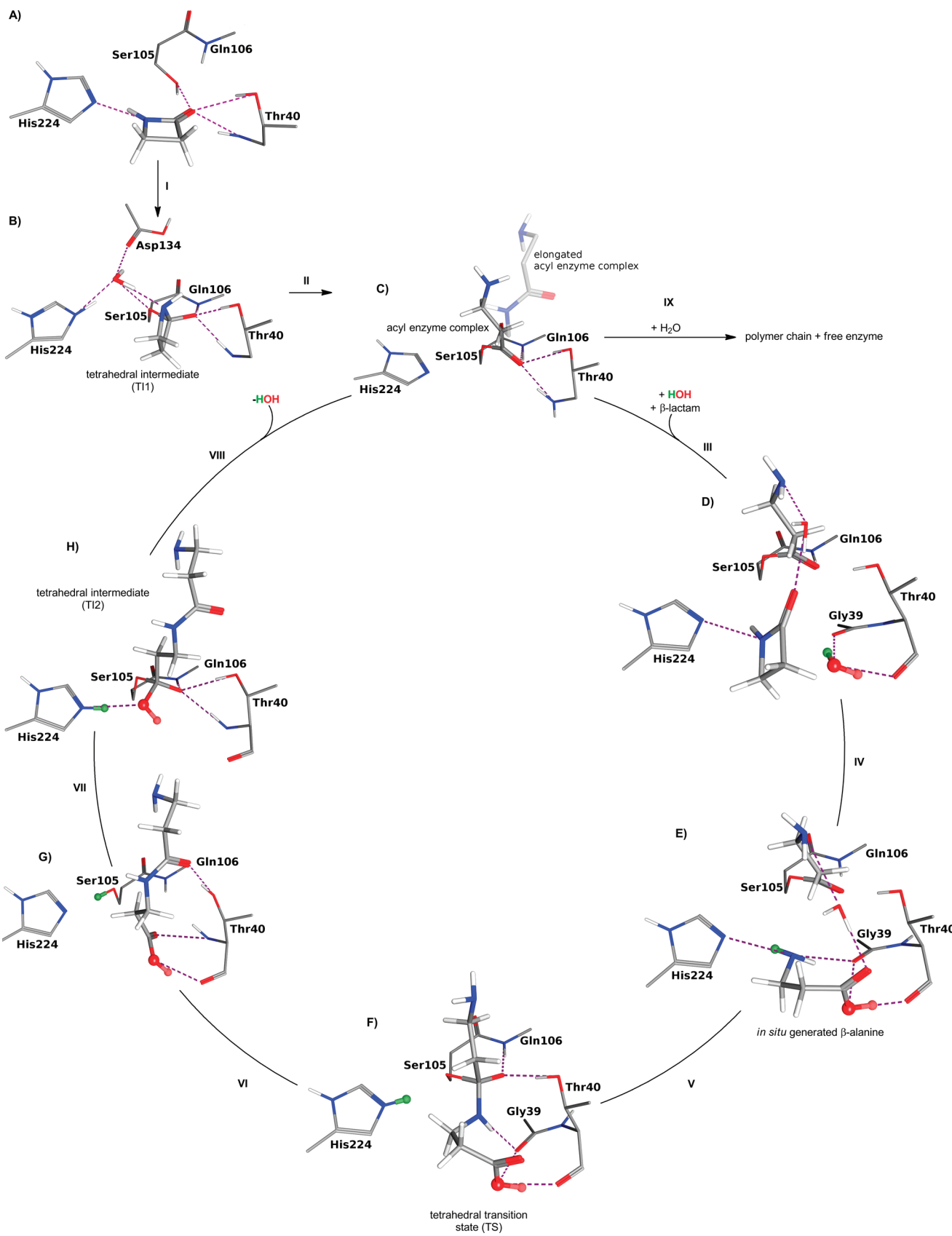
All calculations were based on the crystal structure of *C. antarctica* lipase B complexed with a covalently bound phosphonate inhibitor (PDB ID: 1LBS),³⁰ which can be found in the Brookhaven Protein Data Bank.⁴² The catalytically used water molecule was extracted from the crystal structures of the native *C. antarctica* lipase B (PDB ID: 1TCA, 1TCB),³⁸ inserted in 1LBS, and energy-minimized. Protein preparation for docking simulations was done with the program MOE.⁴³ All water molecules, ligands, and non-protein residues were deleted if not mentioned otherwise. The crystallographic water molecules were inserted afterward in their energy-minimized positions if needed for the reaction.

For pK_a calculations of β -alanine and its oligomers, we employed the ACD/PhysChem Suite from ACD/Laboratories which predicts physicochemical properties applying fragment-based models.³³ The pK_a calculations of ligands inside the active side of *C. antarctica* lipase B were carried out utilizing the PROPKA Web Interface (Version 2.0).³⁴ Because PROPKA assumes a pK_a value of 4.50 in water for all carboxylic acids, the calculations were rerun with experimental pK_a values or, in the case of the β -alanine dimer, values predicted by the ACD/PhysChem Suite.

Docking studies were performed using the program QXP-Flo (Quick eXPlore)⁴⁴ using a sphere of 15 Å around the active site as the model system. The docking volume is always to be defined manually by adequate coloration of guided atoms. All protein residues are held fixed except for the catalytic water molecule, the catalytical histidine and serine, and the oxyanion hole (His224–N or His224–NH, Ser105–OH or Ser105–O, Gln106–NH, Thr40–NH, and Thr40–OH). In the case of an acylated enzyme, the amino group and carbonyl oxygen of the acyl chain were also unfixed during docking of a second ligand. The unfixed hetero atoms were allowed a constrained movement of 2 Å; the attached polar hydrogens were allowed to move freely. In general, docking experiments were carried out in the absence of water because the water oxygen is constrained in its movement (max 2 Å), and the water may not be able to diffuse away if a space-consuming ligand enters the pocket. If docking runs are performed in the presence of a catalytic water molecule, a subsequent energy minimization is particularly important to give the water molecule the chance to possibly diffuse out of an energetically unfavorable position. All structures (with and without water) run through a refinement procedure of several energy minimizations after docking.

At the start of a docking experiment, the ligand is first placed manually outside the binding region and positioned inside the active side by the sdock tool included in QXP. The ligand is placed without conformational search in an adequate starting position for the following docking runs. This starting conformation is used for a full Monte Carlo search (mcdock) from which the rescored docking hits run through a local Monte Carlo search (mlcdock) with limited degrees of freedom for further refinement. For rescoring of docking results, the method of Alisaraie

Scheme 3. Catalytic Cycle of CALB-Mediated Polymerization of β -Lactam Consisting of Steps I and II (Acylation of Ser105 by β -Lactam), Step III (Positioning of a Second Molecule of β -Lactam for Chain Elongation), Step IV (In Situ Generation of β -Alanine As the Chain-Elongating Monomer), Step V (Attachment of β -Alanine to the Acylated Serine), Step VI (Positioning of the Dimer for Further Elongation), Steps VII and VIII (Acylation of Serine by the Dimer), and Step IX (Liberation of the Polymer from the Enzyme)



et al.⁴⁵ in combination with a principal component analysis was used.

The crystal structure 1LBS is prepared as already described and protonated afterward using the protonate3D tool from MOE. In addition, similarly to the studies of Garcia-Urdiales et al.,⁴⁶ Asp134 is protonated manually because a deprotonation of Asp134 destroys the internal hydrogen bonding network of the protein and causes a destabilization of the oxyanion hole as the hydroxyl group of Thr40 drifts outward. It has been shown, however, that this does not change the general findings of the CALB-catalyzed β -lactam polymerization.²⁹ The docked structures were aligned with this prepared structure of 1LBS, and the ligand was transferred to this structure to gain a complete and uncut enzyme model.

Docking results were then refined by a cascade of energy minimizations using MOE. First, the hydrogen atoms of the protein were minimized using the Amber99 force field⁴⁷ while all heavy atoms and the ligand were held fix. In the second and the third minimization steps, the protein side chains and the complete protein were released. The last minimization step contains the ligand, a catalytic water molecule (if present), and a sphere of 7 Å around the ligand as a flexible domain on which the MMFF94x force field is applied while the rest of the protein is held fixed. Refined docking results were used for molecular dynamics runs and QM/MM geometry optimizations.

Molecular dynamics simulations were carried out with MOE using the NPT ensemble and the Nosé–Poincaré–Anderson (NPA) equations. The simulation was run for 1 ns at a temperature of 300 K and a pressure of 101 kPa. A step size of 0.001 ps was selected, and no bond constraints were applied.

All QM/MM geometry optimizations were performed employing the NWChem package (Version 6.0, Pacific Northwest National Laboratory, USA).^{39,40} The residues of the active side (Ser105, Gln106, Thr40, His224) and those that are important for the stabilization of the oxyanion hole (Asp134, Gln157) were part of the QM region; the residual enzyme and the protein were included in the MM subsystem. The QM/MM boundary carbons were capped with H atoms and treated by the pseudo bond approach.^{48,49} The QM region uses DFT quantum chemical methods at the B3LYP level with the Ahlrichs-pVQZ basis set, and the AMBER99 force field is applied for the MM part. Proton transfers in the QM region can be induced by the “spring method” of NWChem, which applies a harmonic restraint between a donated proton and a proton acceptor and drives the starting configuration to the closest product state while at the same time allowing the MM system to adjust to the changes. When a reasonable estimate of a given proton transfer is obtained, the constraint is lifted, and the system is allowed to relax using a sequence of optimization and dynamical relaxation steps. For our calculations a spring length of 1.8 au (~ 0.95 Å) was applied for the proton transfer between the proton and the accepting heteroatom of the target (His224 and Ser105) with a force constant of 0.5 au.

To model the first three stages of the catalytic cycle in toluene, COSMO (conductor-like screening model) calculations⁵⁰ were performed to describe dielectric screening effects in solvent, as implemented into the software packet of NWChem. In the current implementation, the code calculates the gas-phase energy of the system, followed by the solution-phase energy, and returns the electrostatic contribution to the solvation free energy. The toluene solvent was approximated by a dielectric continuum in which the dielectric constant was set to 2.38. The size of the

system was limited to the size of QM region, where the atoms of the former QM/MM boundary were held fix during COSMO calculations.

AUTHOR INFORMATION

Corresponding Author

*Phone: (+49) 5251-60-2181. Fax: (+49) 5251-60-3245. E-mail: fels@upb.de.

ACKNOWLEDGMENT

This work was supported by the German Science Foundation (DFG), under Contract No. FE 170/10-1. Iris Baum thanks the German Academic Exchange Service (DAAD) for financial support of her research stay at the University of Groningen. The authors thank Prof. Dr. Ulrich Jordis (Vienna University of Technology, Institute of Applied Synthetic Chemistry) for the calculation of pK_a values. QM/MM calculations were carried out at the Paderborn Center for Parallel Computing and at the Pacific Northwest National Laboratory using EMSL, a national scientific user facility sponsored by the Department of Energy’s Office of Biological and Environmental Research.

REFERENCES

- (1) Anderson, E. M.; Larsson, K., M.; Kirk, O. *Biocatal. Biotransform.* **1998**, *16* (3), 181–204.
- (2) Kobayashi, S.; Uyama, H.; Kimura, S. *Chem. Rev.* **2001**, *101*, 3793–3818.
- (3) Kobayashi, S.; Ritter, H.; Kaplan, D. Enzyme-Catalyzed Synthesis of Polymers. In *Advances in Polymer Science*; Springer: Berlin, 2006, ISBN 0065-3195, DOI 10.1007/11549307.
- (4) Binns, F.; Harffey, P.; Roberts, S. M.; Taylor, A. *J. Polym. Sci., Part A: Polym. Chem.* **1998**, *36* (12), 2069–2079.
- (5) Gross, R. A.; Kumar, A.; Kalra, B. *Chem. Rev.* **2001**, *101* (7), 2097–2124.
- (6) Uyama, H.; Kobayashi, S. *Enzyme-Catal. Synth. Polym.* **2006**, *194*, 133–158.
- (7) Jääskeläinen, S.; Linko, S.; Raaska, T.; Laaksonen, L.; Linko, Y. Y. *J. Biotechnol.* **1997**, *52* (3), 267–275.
- (8) Varma, I. K.; Albertsson, A.-C.; Rajkhowa, R.; Srivastava, R. K. *Prog. Polym. Sci.* **2005**, *30*, 949–981.
- (9) Al-Azemi, T.; Kondaventi, L.; Bisht, K. *Macromolecules* **2002**, *35*, 3380–3386.
- (10) Kikuchi, H.; Uyama, H.; Kobayashi, S. *Macromolecules* **2000**, *33*, 8971–8975.
- (11) Kumar, A.; Gross, A. *Biomacromolecules* **2000**, *1*, 133–138.
- (12) Matsumura, S. *Adv. Polym. Sci.* **2006**, *194*, 95–132.
- (13) Mei, Y.; Kumar, A.; Gross, R. *Macromolecules* **2003**, *36* (15), 5530–5536.
- (14) Thurecht, K. J.; Heise, A.; deGeus, M.; Villarroya, S.; Zhou, J. X.; Wyatt, M. F.; Howdle, S. M. *Macromolecules* **2006**, *39* (23), 7967–7972.
- (15) van der Mee, L.; Helmich, F.; de Bruijn, R.; Vekemans, J. A. J. M.; Palmans, A. R. A.; Meijer, E. W. *Macromolecules* **2006**, *39*, 5021–5027.
- (16) Cheng, H. N.; Maslanka, W. W.; Gu, Q.-M., U.S. Patent 6677427, 2004; Hercules Inc, invs.
- (17) Gu, Q.-M.; Maslanka, W. W.; Cheng, H. N. *Polymer Biocatalysis and Biomaterials II*; Cheng, H. N., Gross, R. A., Eds.; ACS Symposium Series, **2008**, 999, Chapter 21, pp 309–319.
- (18) Schwab, L. W.; Kroon, R.; Schouten, A. J.; Loos, K. *Macromol. Rapid Commun.* **2008**, *29*, 794–797.
- (19) Haeffner, F.; Norin, T. *Chem. Pharm. Bull.* **1999**, *47* (5), 591–600.

- (20) Kobayashi, S. *Macromol. Rapid Commun.* **2009**, *30* (4–5), 237–266.
- (21) Park, S.; Forro, E.; Grewal, H.; Fulop, F.; Kazlauskas, R. I. *Adv. Synth. Catal.* **2003**, *345* (8), 986–995.
- (22) Adam, W.; Groer, P.; Humpf, H.-U.; Saha-Möller, C. R. *J. Org. Chem.* **2000**, *65*, 4919–4922.
- (23) Forro, E.; Fulop, F. *Org. Lett.* **2003**, *5* (8), 1209–1212.
- (24) Tasnadi, G.; Forro, E.; Fülop, F. *Tetrahedron: Asymmetry* **2007**, *18*, 2841–2844.
- (25) Hollmann, F.; Grzebyk, P.; Heinrichs, V.; Doderer, K.; Thum, O. *J. Mol. Catal. B: Enzym.* **2009**, *57* (1–4), 257–261.
- (26) Dash, U. N.; Nayak, S. K. *Can. J. Chem., Rev. Can. Chim.* **1980**, *58* (10), 992–995.
- (27) Mahapatro, A.; Kumar, A.; Kalra, B.; Gross, R. A. *Macromolecules* **2004**, *37* (1), 35–40.
- (28) Tarabek, P.; Bonifacic, M.; Beckert, D. *J. Phys. Chem. A* **2006**, *110* (22), 7293–7302.
- (29) Schwab, L. W.; Baum, I.; Fels, G.; Loos, K. In *Green Polymer Chemistry: Biocatalysis and Biomaterials*; Cheng, H. N., Gross, R. A., Eds.; ACS Symposium Series; American Chemical Society: Washington DC, **2010**; in press.
- (30) Uppenberg, J.; Ohrner, N.; Norin, M.; Hult, K.; Kleywegt, G. J.; Patkar, S.; Waagen, V.; Anthonsen, T.; Jones, T. A. *Biochemistry* **1995**, *34* (51), 16838–16851.
- (31) Kobayashi, S. *Macromol. Symp.* **2006**, *240*, 178–185.
- (32) Panova, A. A.; Kaplan, D. L. *Biotechnol. Bioeng.* **2003**, *84* (1), 103–113.
- (33) http://www.acdlabs.com/products/pc_admet/physchem/physchemsuite/ (Accessed February 22, 2011).
- (34) Bas, D. C.; Rogers, D. M.; Jensen, J. H. *Proteins* **2008**, *73*, 765–783.
- (35) Veld, M. A. J.; Fransson, L.; Palmans, A. R. A.; Meijer, E. W.; Hult, K. *ChemBioChem* **2009**, *10* (8), 1330–1334.
- (36) Gonzalez-Sabin, J.; Lavandera, I.; Rebollo, F.; Gotor, V. *Tetrahedron: Asymmetry* **2006**, *17* (8), 1264–1274.
- (37) Lavandera, I. W.; Fernandez, S.; Magdalena, J.; Ferrero, M.; Kazlauskas, R. J.; Gotor, V. *ChemBioChem* **2005**, *6* (8), 1381–1390.
- (38) Uppenberg, J.; Hansen, M. T.; Patkar, S.; Jones, T. A. *Structure* **1994**, *2* (4), 293–308.
- (39) Kendall, R.; Apra, E.; Bernholdt, D.; Bylaska, E.; Dupuis, M.; Fann, G.; Harrison, R.; Ju, J.; Nichols, J.; Nieplocha, J.; Straatsma, T.; Windus, T.; Wong, A. *Comput. Phys. Commun.* **2000**, *128*, 260–283.
- (40) Valiev, M.; Yang, J.; Adams, J.; Taylor, S.; Weare, J. *J. Phys. Chem. B* **2007**, *111* (47), 13455–13464.
- (41) El Firdoussi, A.; Esseffar, M.; Bouab, W.; Abboud, J. M.; Mo, O.; Yanez, M.; Ruasse, M. F. *J. Phys. Chem. A* **2005**, *109*, 9141–9148.
- (42) Berman, H. M.; Westbrook, J.; Feng, Z.; Gilliland, G.; Bhat, T. N.; Weissig, H.; Shindyalov, I. N.; Bourne, P. E. *Nucleic Acids Res.* **2000**, *28*, 235–242.
- (43) MOE, <http://www.chemcomp.com/>, 2010.09 (Accessed February 22, 2011).
- (44) McMartin, C.; Bohacek, R. S. *J. J. Comput.-Aided Mol. Des.* **1997**, *11*, 333–344.
- (45) Alisaraie, L.; Haller, L. A.; Fels, G. *J. Chem. Inf. Model.* **2006**, *46*, 1174–1187.
- (46) Garcia-Urdiales, E.; Rios-Lombardia, N.; Mangas-Sanchez, J.; Gotor-Fernandez, V.; Gotor, V. *ChemBioChem* **2009**, *10* (11), 1830–1838.
- (47) Wang, J.; Cieplak, P.; Kollman, P. A. *J. Comput. Chem.* **2000**, *21*, 1049–1074.
- (48) Valiev, M.; Garrett, B. C.; Tsai, M. K.; Kowalski, K.; Kathmann, S. M.; Schenter, G. K.; Dupuis, M. *J. Chem. Phys.* **2007**, *127* (5), 51102 (1–4).
- (49) Zhang, Y. K.; Lee, T. S.; Yang, W. T. *J. Chem. Phys.* **1999**, *110* (1), 46–54.
- (50) Klamt, A.; Schüürmann, G. *J. Chem. Soc., Perkin Trans.* **1993**, *2*, 799–805.